

## VUV spectroscopy measurements on WEST first plasmas

C. Desgranges<sup>1</sup>, R. Guirlet<sup>1</sup>, O. Meyer<sup>1</sup>, S. Sangaroon<sup>2</sup>, J.L. Schwob<sup>3</sup>, P. Mandelbaum<sup>3</sup>,  
S. Vartanian<sup>1</sup> & the WEST team (<http://west.cea.fr/WESTteam>)

<sup>1</sup> CEA, IRFM, 13108 St-Paul-Lez-Durance, France

<sup>2</sup> Mahasarakham University, Thailand

<sup>3</sup> Racah Institute of Physics, The Hebrew University, 91904 Jerusalem, Israel

**1. Introduction:** For the first operation phase of the WEST tokamak [1-2], copper Plasma Facing Components (PFC) were directly tungsten coated (upper divertor and baffle) and carbonaceous components were coated with a molybdenum sublayer covered by a tungsten layer (lower inertial divertor, inner and outer limiters, antennae limiters), 6 lower divertor units in 456 were made of W monoblocks [3-5]. A particular attention was paid to the cleanliness of internal components. Particularly each reused element from Tore Supra, including each component before coating, was carefully treated to remove all the deposits it had. Table 1 summarizes WEST start up phases, with the C1 and C2 campaigns.

C1	C2 1 <sup>st</sup> part	C2 2 <sup>nd</sup> part
Magnetic configuration optimization [Nardon O3.110]	Burn-through optimization	Diverted plasmas LH power ramp up [Ekedahl, P5.1048]
Ip max=90kA	Ip max~ 300kA	Ip max=800kA
Plasma duration <0.3 s		Up to 10 s
> #50000	> #51800	≥#52202

Table 1: WEST start up phases

In this paper, the core plasma impurity content measured by a VUV spectrometer already existing on Tore Supra are presented [6-9]. Thanks to two detectors, it allows simultaneous acquisition of two wavelength intervals within the total range 0.5 to 34 nm permitted by the grating used here [10]. The spectrometer line of sight was kept fixed viewing in the plasma

midplane. It is to be noted that all processed spectra were normalized to the volume average electron density  $\langle n_e \rangle$  [11].

## 2. Experimental results: Light impurities

### 2.1. Carbon

Due to specific precautions mentioned above the carbon content was expected to drop significantly compared to the previous Tore Supra carbon configuration. Indeed this was the case during the C1 campaign. No carbon signal was observed during the C1 campaign. The C V doublet lines at 4.03 and 4.07 nm appeared during the first part of the C2 campaign, after runaway electrons impact on the inner and outer limiters. Then nearly a week of operation later, the C VI Ly  $\alpha$  line at 3.34 nm appeared thanks to increasing plasma temperature (indeed C V maximum fractional abundance is around 10-70 eV and C VI is around 100 eV) (figure 1).

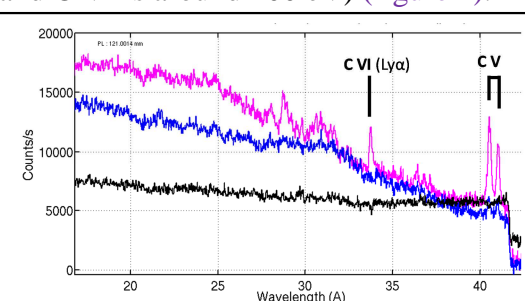
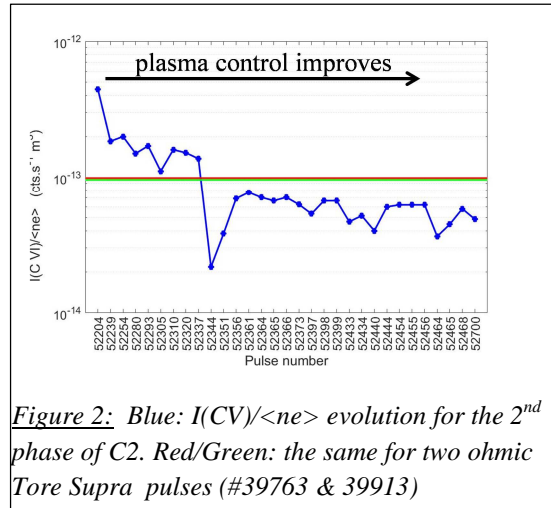


Figure 1: Raw spectrum of #51513 (black)  
#51931 (blue) and #51970 (pink)

From then on, carbon lines were observed in every pulse. Their intensity increased until the first X point on the lower divertor was achieved, in the 2<sup>nd</sup> phase of C2 (#52239). Then as the control of the

plasma position improved, the normalised C VI Ly  $\alpha$  line intensity  $I(C VI)/\langle n_e \rangle$  decreased to a lower limit around  $4.10^{-14}$  cts.s $^{-1}$ m $^3$  as shown in [figure 2](#). This figure also presents two horizontal lines showing the level recorded during two ohmic pulses of Tore Supra (with carbonaceous walls), performed in conditions similar to WEST:  $I_p=600$  kA,  $n_e \approx 1.10^{19}$  m $^{-2}$  ( $n_e \approx 1.5.10^{19}$  m $^{-2}$  typically in WEST).



[Figure 2](#): Blue:  $I(C VI)/\langle n_e \rangle$  evolution for the 2<sup>nd</sup> phase of C2. Red/Green: the same for two ohmic Tore Supra pulses (#39763 & 39913)

It could be deduced that the WEST carbon line is between a factor of 2 to 4 less than in Tore Supra.

To reduce the carbon pollution of the plasma, damaged coated tiles were replaced with new tiles or swapped with less damaged tiles for the C3 campaign.

## 2.2. Oxygen

The first evidence of the O VIII Ly  $\alpha$  line at 1.9 nm appears two experimental days after carbon lines of #51970 ([figure 3](#)).

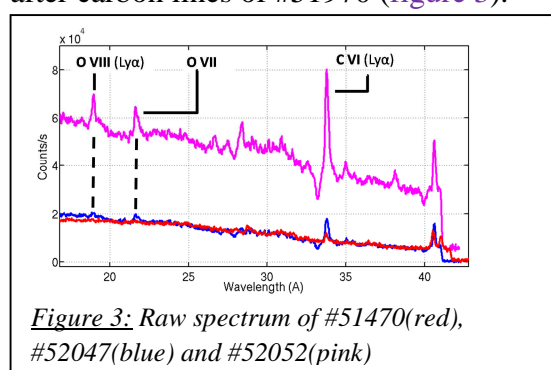


[Figure 3](#): Raw spectrum of #51470(red), #52047(blue) and #52052(pink)

As O VIII maximum fractional abundance is around 200 eV, this could be an

indication that plasma temperature increases. The evolution of  $I(O VIII)/\langle n_e \rangle$  at 1.9 nm during the 2<sup>nd</sup> phase of C2 is shown in [figure 4](#). The oxygen level was nearly constant around  $1.10^{-13}$  cts.s $^{-1}$ m $^3$  until it drops thanks to the plasma position control improvements. Then it remains roughly constant around  $3-4.10^{-14}$  cts s $^{-1}$ m $^3$ .

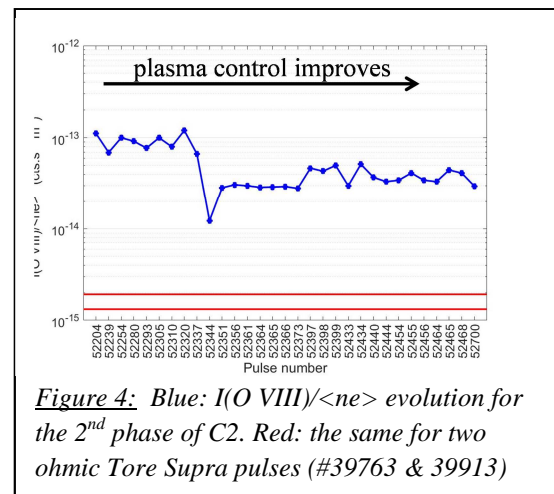


[Figure 4](#): Blue:  $I(O VIII)/\langle n_e \rangle$  evolution for the 2<sup>nd</sup> phase of C2. Red: the same for two ohmic Tore Supra pulses (#39763 & 39913)

The normalized intensity  $I(O VIII)/\langle n_e \rangle$  of the same two Tore Supra pulses presented on [figure 2](#) are represented by two horizontal lines. It can be seen that the WEST oxygen line is more than one order of magnitude higher than during Tore Supra (which was well conditioned and where boronizations were performed). This high level of oxygen is likely to contribute largely to the plasma radiative power which remained quite elevated during all the operation duration. 90% of the power was radiated in ohmic and down to 45% during LHCD [12].

## 3. Experimental results: Metal impurities

Copper, iron and nickel impurities were already monitored in Tore Supra. Molybdenum and tungsten are new impurities due to the new WEST PFC materials. Here we focus on copper and tungsten observations.

### 3.1. Copper

First evidence of the Cu XIX line at 27.34 nm appears a few experimental days after O VIII was established. As Cu XIX maximum fractional abundance is around 350 eV, this could be again an indication of plasma temperature increase. In the carbon environment machine, copper lines were generally observed only when breakdowns and arcs occurred at the mouth of the Lower Hybrid (LH) launcher. During WEST operation, the LH power was ramped up to 2.5 MW [12]. Copper line evolution presented here is restricted to 1.2 MW LH due to a change in detector wavelength setting. Nevertheless the main result of this evolution is the increase of  $I(\text{Cu XIX})/\langle n_e \rangle$  with the LH power (figure 5).

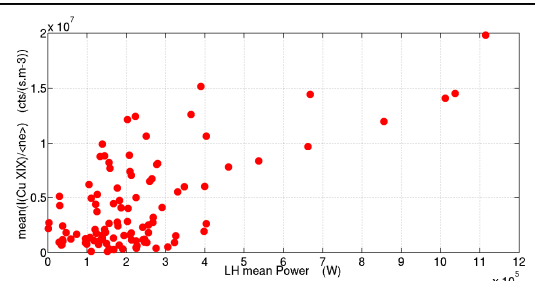


Figure 5: Average  $I(\text{Cu XIX})/\langle n_e \rangle$  versus average LH power in watt

One hypothesis to explain this observation could be that copper previously deposited on walls by other events (conditioning by glow discharge, runaway electron impact), is re-mobilized during LH heated pulses. The copper line intensity increases also during the first second of plasma when it is leaning on the inner bumpers (figure 6).

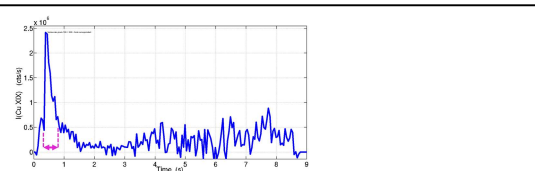


Figure 6: Time evolution of  $I(\text{Cu XIX})$  (e.g. #52469 pulse). Pink: leaning on inner bumper

The evolution of this first second  $I(\text{Cu XIX})/\langle n_e \rangle$  value averaged over each experimental day is presented on figure 7.

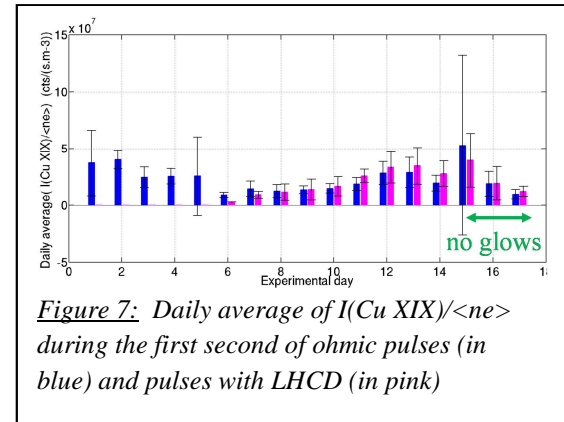


Figure 7: Daily average of  $I(\text{Cu XIX})/\langle n_e \rangle$  during the first second of ohmic pulses (in blue) and pulses with LHCD (in pink)

Within the same day, ohmic pulses were averaged independently of pulses including LH heating. No difference is observed between ohmic and LH heated pulses on the copper intensity during the first second of the plasma. In the 2<sup>nd</sup> part of C2, glow discharges took place each morning and each evening except the last three days of experiments reported here during which a decrease by more than 50% is noticeable. Apart from the first second and during the LH time window the copper line intensity was roughly divided by a factor of two over the 17 days of the 2<sup>nd</sup> part of C2 studied here.

### 3.2. Tungsten

To perform tungsten spectroscopy measurements, various spectral ranges were selected. Firstly in the 3.5-7.5 nm range an increasing feature correlated to the LH heating was observed (figure 8).

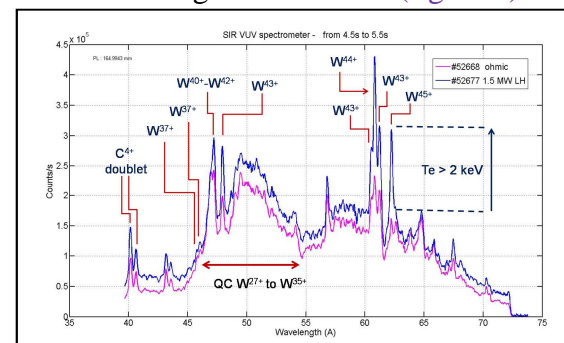


Figure 8: In Pink: Raw spectrum of ohmic #52668 – In Blue: Spectrum of #52677 with 1.5MW LHCD. Identified lines are reported on the figure.

During the 2<sup>nd</sup> phase of C2, the core electron temperature was increased from 300 eV (ohmic case) to more than 2 keV (as confirmed by the ECE electron temperature measurements). In the same time thorough line identification was undertaken.

The last day of operation, the detector was again moved to the 11.5-15.5 nm spectral range. New thorough line identification was undertaken (figure 9).

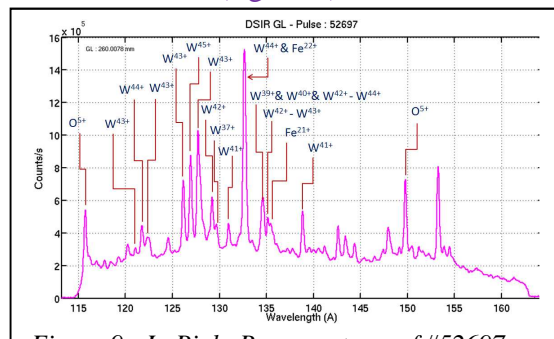


Figure 9: In Pink: Raw spectrum of #52697 during LHCD pulse (2 MW injected at the most). Identified lines are reported on the figure.

It is consistent with previous observations on AUG [13].

#### 4. Conclusion

First results were obtained with the VUV spectrometer during the first 2 WEST campaigns. During the burn-through optimization, due to frequent runaway beams, carbon lines appeared and reached levels a factor 2-4 lower than in Tore Supra. In the phase with X point operation the oxygen level was an order of magnitude higher than in the previous Tore Supra carbon environment. During this phase, unusually strong copper lines appeared during the first second of plasma while leaning on the inner bumpers and independently whether LH heating was previously applied. Stopping glow discharges resulted in a 50% decrease of

the Cu XIX intensity in the first second plasma.

Also the copper intensity increases with power during LH heating window.

First lines of tungsten were observed to become stronger with increasing plasma temperature. The spectrum shape and the line identification are in satisfactory agreement with previous observations on AUG in the range 11.5 to 14 nm.

Line identification is still underway particularly concerning molybdenum.

**Acknowledgements:** The authors want to thank Dr Pascale Monier-Garbé for her help to interpret results in this new tungsten environment and new plasma configuration.

## References:

- [1] J. Bucalossi et al., Fusion Eng. Des. 86 (2011) 684-688
- [2] A. Grosman et al., Fusion Eng. Des. 88 (2013) 497-500
- [3] M. Firdaouss et al., 2016 Phys. Scr. 2016 014012
- [4] M. Richou et al., 2016 Phys. Scr. 2016 014029
- [5] C. Desgranges et al., 2016 Phys. Scr. 2016 014060
- [6] O. Meyer et al., J. of Nucl Mat 390–391 (2009) 1013–1016
- [7] R. Guirlet et al., 30<sup>th</sup> EPS Conference on Controlled Fusion and Plasma Physics, St-Petersburg, 2003
- [8] P. MonierGarbet et al., Plasma Phys. and Contr. Nucl. Fus. Res. IAEA **Vol 1** (1992) 317-322 ISBN: 92-0-101093-1
- [9] C. Gil et al., Fus. Science and Tech. **56** N°3 (2009) 1219-1252 ; ISSN : 1536-1055
- [10] J.L. Schwob et al., Rev. Sci. Instrum.**58**, (1987) 1601; doi: 10.1063/1.1139408
- [11] O. Meyer et al., J. Nucl. Mat. **390–391** (2009) 1013–1016
- [12] A. Ekedahl et al., this conference P5-1048
- [13] T. Pütterich et al., 2008 Plasma Phys. Control. Fusion 50 085016